Astron. Astrophys. 336, 667–681 (1998)

ASTRONOMY AND ASTROPHYSICS

The planetary nebulae populations in five galaxies: abundance patterns and evolution⋆

G. Stasińska[1], **M.G. Richer**[2], **and M.L. Mc Call**[3]

[1] DAEC, Observatoire de Paris-Meudon, F-92195 Meudon Cedex, France (grazyna@obspm.fr)
[2] Instituto de Astronomía, Universidad Nacional Autónoma de México, Apdo. Postal 70 264, México D.F. 04510, México (richer@astroscu.unam.mx)
[3] Department of Physics and Astronomy, York University, 4700 Keele Street, North York, Ontario, Canada M3J 1P3 (mccall@aries.phys.yorku.ca)

Received 3 March 1998 / Accepted 19 May 1998

Abstract. We have collected photometric and spectroscopic data on planetary nebulae (PNe) in 5 galaxies: the Milky Way (bulge), M 31 (bulge), M 32, the LMC and the SMC.

We have computed the abundances of O, Ne and N and compared them from one galaxy to another. In each Galaxy, the distribution of oxygen abundances has a large dispersion. The average O/H ratio is larger in the M 31 and the Galactic bulge PNe than in those in the Magellanic Clouds. In a given galaxy, it is also larger for PNe with [O III] luminosities greater than 100 $L_{\odot}$, which are likely to probe more recent epochs in the galaxy history. We find that the M 31 and the Galactic bulge PNe extend the very tight Ne/H–O/H correlation observed in the Galactic disk and Magellanic Clouds PNe towards higher metallicities. We note that the anticorrelation between N/O and O/H that was known to occur in the Magellanic Clouds and in the disk PNe is also marginally found in the PNe of the Galactic bulge. Furthermore, we find that high N/O ratios are higher for less luminous PNe. In M 32, all PNe have a large N/O ratio, indicating that the stellar nitrogen abundance is enhanced in this galaxy.

We have also compared the PN evolution in the different galactic systems by constructing diagrams that are independent of abundances, and have found strikingly different behaviours of the various samples.

In order to help in the interpretation of these data, we have constructed a grid of expanding, PN photoionization models in which the central stars evolve according to the evolutionary tracks of Blöcker (1995). These models show that the apparent spectroscopic properties of PNe are extremely dependent, not only on the central stars, but also on the masses and expansion velocities of the nebular envelopes.

The main conclusion of the confrontation of the observed samples with the model grids is that the PN populations are indeed not the same in the various parent galaxies. Both stars and nebulae are different. In particular, the central stars of the Magellanic Clouds PNe are shown to evolve differently from the hydrogen burning stellar evolutionary models of Blöcker (1995). In the Galactic bulge, on the other hand, the behaviour of the observed PNe is roughly compatible with the theoretical stellar evolutionary tracks. The case of M 31 is not quite clear, and additional observations are necessary. It seems that the central star mass distribution is narrower for the M 31 PNe than for the Galactic bulge PNe.

We show that spectroscopy of complete samples of PNe down to a factor 100 below the maximum luminosity would help to better characterize the PN central star mass distribution.

Key words: ISM: planetary nebulae: general – stars: AGB and post-AGB – galaxies: abundances.

1. Introduction

There is a rapidly growing body of observational data on planetary nebulae (hereinafter PNe) in different galaxies (see e.g. Jacoby 1998). The most pressing motivation is the determination of the distances of galaxies through the PN luminosity function. This technique relies on the observation that the upper part of the PN luminosity function is independent of the host galaxy. Why this is so is actually a matter of debate, and several recent papers have addressed this question from different perspectives (Jacoby 1989, Dopita et al. 1992, Méndez et al. 1993, Méndez & Soffner 1997, Richer et al. 1997). Spectroscopic data on large samples of PNe in different galaxies allow a deeper insight into this question, as they provide more information on the physics of the PNe and their central stars. In such a way, they make it possible to probe the stellar evolution of post-AGB stars during the PN phase, and to get an idea of the population of stars responsible for the PN phenomenon in a given galaxy.

Recently, we have obtained spectra of a sample of luminous PNe in the bulge of M 31 and in M 32 (Richer et al. 1998a). Together with published observations of PNe in the Galactic bulge and in the Magellanic Clouds, this offers the possibility

Send offprint requests to: Stasińska

⋆ Tables 1 and 2 are only available in electronic form at the CDS via anonymous ftp to cdsarc.u-strasbg.fr (130.79.128.5) or via http://cdsweb.u-strasbg.fr/Abstract.html

of a comparative study of the PN populations in five galaxies of different types.

The paper is organized as follows. In Sect. 2, we describe our data base, and the procedure used to derive ionic and atomic abundances from PN spectra. In Sect. 3, we compare the abundance patterns obtained for the PNe in the different galaxies. In Sect. 4, we present observational diagrams linked to the central star properties and to the evolutionary status of the nebulae, and state the observed differences among the various galaxies. In Sect. 5, we show, in the same coordinates, the evolutionary tracks of models of PNe based on post AGB stellar tracks and photoionization calculations of the surrounding expanding nebulae, and we comment on the main predictions of the models. In Sect. 6, we discuss the observational diagrams in the light of the models. The conclusions are summarized in Sect. 7.

2. The database

2.1. Collecting the data

The line intensities for the M 31 and M 32 samples are taken from Richer et al. (1998a): they concern 28 bright PNe in the bulge of M 31 (plus 2 in the disk of M 31 seen in projection on M 32), and 9 in M 32. For these objects, the [O III] magnitudes are taken from Ciardullo et al. (1989). The adopted distance modulus of M 31 and M 32 is 24.286 mag (Richer & Mc Call, 1995). The data do not allow an accurate determination of the reddening in most of the cases. However, extinction internal to M 31 is not expected to be important for the PNe of our sample, since they lie in the bulge. This is confirmed by the rather small value of the extinction (E(B-V) < 0.20 mag; Richer et al. 1998a) for the objects for which we could measure the Hα/Hβ ratio. The observed luminosities in [O III] were corrected for foreground Galactic extinction, using $E(B-V) = 0.093$ mag as in Richer & Mc Call (1995)

For the Magellanic Cloud samples (LMC and SMC), we used the line intensities corrected for reddening from the sources listed in Richer & Mc Call (1995) to which we added Leisy & Dennefeld (1996), and the [O III] magnitudes adopted by these authors. The PNe are assumed to be at distance moduli of 18.372 and 18.85 mag in the LMC and SMC, respectively (Richer & Mc Call 1995)[1]. The [O III] luminosities of the PNe in the LMC and SMC have been corrected for foreground extinctions corresponding to (E(B-V) of 0.019 mag and 0.035 mag, respectively (Richer & Mc Call 1995). We considered using the reddenings derived for individual PN spectra, but chose not to since the c(Hβ) values in the literature for any particular object often span a range of 0.2 to 0.3 dex or more.

For the Galactic bulge sample, we used the spectroscopic data of Aller & Keyes (1987), Webster (1988) and Ratag et al. (1997). In the case of multiple spectroscopic observations of the same object, we adopted the data which seemed more reliable. We kept only the objects for which there was at least a measurement of [O III]5007 or [O II]3727 or [O II]7325 in addition to Hβ. The line intensities were already corrected for reddening in the original papers. The Hβ or radio fluxes were taken from the sources listed in Stasińska et al. (1992), and the Hβ fluxes were corrected for extinction adopting the prescription given in that paper. In order to reduce the proportion of PNe that are seen in projection in the bulge, but do not pertain physically to it, we have rejected from the sample all the PNe whose radio flux at 6 cm was larger than 100 mJy. When no flux measurement was available, we assumed the PNe to be fainter than this limit. With such a procedure, 90-95 % of PNe of the sample should be located physically in the bulge (Stasińska et al. 1991).

The reddening corrected line intensities relative to Hβ for all the PNe we consider are reported in Table 1 [2], together with the adopted luminosities in [O III]5007, $L_{[\mathrm{O\,III}]}$ (in solar units). There are 30 objects for M 31, 9 objects for M 32, 90 objects for the Galactic bulge (that fulfil the condition on the Hβ luminosity), 139 objects for the LMC and 61 objects for the SMC. Note that values of $L_{[\mathrm{O\,III}]}$ are not available for all the objects.

The quality of the data in the samples is not uniform, even in a single galaxy (see Jacoby & Kaler 1993 for a discussion of some of the quality issues in the Magellanic Clouds PNe). On average, the quality is expected to be better for the high luminosity objects.

2.2. Plasma diagnostics and determination of abundances

All the PN spectra were processed in the same way, using standard empirical methods with the atomic data listed in Stasińska & Leitherer (1996) in order to derive the ionic and elemental abundances.

In all the cases, the ionic abundances were derived using the electron temperature from the [O III] 4363/5007 ratio (or from the [N II]5755/6584 one if the former was not available). For a number of objects, especially in M 31 and M 32, only upper limits to the [O III]4363 intensity are available, leading to upper limits for the electron temperatures, and lower limits for the ionic abundances of the heavy elements relative to hydrogen. In some cases (13 out of 90 in the Galactic bulge, 31 out of 139 in the LMC and 13 out of 61 in the SMC), the available data do not give even an upper limit to the electron temperature. For the LMC and the SMC, we simply discard these objects from our abundance analysis, since they constitute a small fraction of the total and it is not likely that their abundance distribution should be different from the rest. In the Galactic bulge, the situation is different. There, we expect some of the PNe to have high metallicities, so the objects lacking [O III]4363 might be precisely the

[1] In Richer & Mc Call (1995), the distances adopted for the Magellanic Clouds and M 31 are anchored to the determination of the distance of SN 1987A. A revised distance to SN 1987 A (Panagia et al. 1998, BAAS 191, 19.09) increases the adopted distance moduli by 0.21 mag, and therefore increases the PN luminosities by about 20%. Such a change is insignificant for the diagrams and the conclusions reported in the present paper.

[2] Tables 1 and 2 are accessible only in electronic form, at the CDS via anonymous ftp to cdsarc.u-strasbg.fr (130.79.128.5) or via http://cdsweb.u-strasbg.fr/Abstract.html.

most metal-rich. In order to check this idea, we have assigned an upper limit of one hundredth of Hβ for the [O III]4363 intensity in these objects. This allows us to estimate a rough lower limit of the abundances in 8 of these objects. The remaining five have so low [O III]5007 fluxes that such a procedure did not lead to an estimate of the temperature. These are probably very metal rich objects. Concerning the electron density, when it was not possible to derive it from [S II]6716/6730, a value of 4 000 cm^{-3} was adopted. The O^+/H ratio was obtained from [O II]3727/Hβ (or [O II]7325/Hβ, when [O II]3727 is not seen, which is the case of 14 of the PNe in the Galactic bulge).

The abundances of O, N and Ne were computed from the ionic abundances using the ionization correction factors of Kingsburgh and Barlow (1994), which are based on detailed photoionization models of 10 PNe. Using these ionization correction factors returns smaller oxygen abundances than when using the classical recipe (adopted for instance by Monk et al., 1988, Henry 1989, Richer & McCall 1995) which erroneously assumes that the region containing higher ionization stages than O^{++} is coextensive with the He^{++} region.

The results from the abundance analysis are listed in Table 2 [3]. Column 1 gives the object names, columns 2–5 give the abundances in number relative to hydrogen of He, N, O, and Ne, respectively. Column 6 gives the electron density (per cm^{-3}) deduced from [S II]6716/6730, while columns 7 and 8 give the electron temperatures (in Kelvin) deduced from [O III]4363/5007 and [N II] 5755/6584, respectively. Columns 9–10 give the value of O^+/H deduced from [O II]3727/Hβ and [O II]7325/Hβ respectively. Columns 11–15 list the values of O^{++}/H, N^+/H, Ne^{++}/H, He^+/H and He^{++}/H, respectively.

It is important to have in mind the error bars in the abundance ratios we consider in this paper. A typical error of 20 % in the intensity of the [O III]4363 line (which is the determining line for the accuracy of abundance evaluations) propagates into an error of at most 20 % in O/H, N/O, Ne/O and O^{++}/O^+. If [O III]4363 is not measured, we can get a feeling of how far the abundance ratios may be from the limits we assigned by seeing how much these ratios change when the electron temperature goes from 10 000K to 7 000K: N/O is multiplied by 0.5 if [O II]3727 is used, 0.2 if [O II]7325 is used; Ne/O is multiplied by 1.3; O^{++}/O^+ is multiplied by 0.6 if [O II]3727 is used and by 0.3 if [O II]7325 is used; O/H is multiplied by 3 if one assumes that all the oxygen is in the form of O^{++}.

The effect of an unknown electron density affects only those ratios involving [O II]3727 or [O II]7325. As an illustration, we compute the changes in these ratios when the electron density goes from 10^3 cm^{-3} to 10^4 cm^{-3}. N/O and O^{++}/O^+ change by a factor of 0.5 when using [O II]3727, and 2 when using [O II]7325. So, for example, in the PNe of M 31, where no determination of the electron density could be made, the uncertainty in the O^{++}/O^+ ratio due to this effect should be $\pm$ 25 %.

The [O II]7325 and [O II]3727 lines are simultaneously available for 39 PNe in the Galactic bulge, 45 in the LMC and 20 in the SMC. The values of O^+/H deduced from [O II]7325 tend to be systematically larger than those deduced from [O II]3727. A typical discrepancy is a factor 2-3. The [O II]3727/Hβ ratio is sensitive to the reddening law adopted. But even in the Galactic bulge PNe, where the extinction is large, the effect of choosing a reddening law with a total-to-selective extinction ratio R_v of about 2.7, as inferred by Stasińska et al. (1992), would increase [O II]3727/Hβ by at most 20%. Another problem that might affect [O II]3727 is atmospheric refraction. The [O II]7325 lines present other problems. Night-sky correction is difficult in this region of the spectrum. Besides, the conversion of the [O II]7325 intensity into an ionic abundance is not accurate due to the great dependence of the line emissivity on both the electron temperature and the density. Therefore, it is our feeling that, generally, the abundance of O^+ derived from [O II]3727 is likely to be more accurate. In the 14 PNe of the Galactic bulge where we had to adopt the O^+ abundance from [O II]7325, we thus expect that it might be overestimated typically by a factor 2. However, the influence on O/H should be statistically negligible, since O^{++} dominates over O^+ in most objects.

3. PN abundance patterns in the various galaxies

As is known, the inferences from abundance ratios in PNe are of a different nature according to the elements considered. Oxygen and neon abundances are only slightly modified by nucleosynthesis in the PN progenitors (Forestini & Charbonnel 1997) and thus trace the composition of the material out of which the progenitors were formed. On the other hand, part of the nitrogen seen in PNe has been synthesized in the progenitors and thus bears some information on their nature.

Abundance patterns for O, Ne and N in our 5 galaxies are displayed in Fig. 1, which consists of 5 rows of 3 panels each. Each row corresponds to a different galaxy, whose name is indicated in the bottom right corner of each panel (MW stands for Milky Way). Each column corresponds to a different set of coordinates. The panels of the left column display O/H as a function of $L_{H\beta}$, the total luminosity in Hβ. In the case of M 32, since the observed sample is small, we also represent the three PNe for which the luminosity is not known by assuming $L_{H\beta} = 25$ $L_\odot$ (horizontal "error bars" are shown for these objects). The middle panels display N/O as a function of O/H. The right panels display Ne/H as a function of O/H. In each panel, the total number of observational points is indicated in parentheses.

Within a galaxy, one expects that the PN abundance distributions depend on the range in PN luminosities that are sampled. Indeed, the most luminous PNe are likely to have rather massive central stars (see Sect. 5), and therefore massive progenitors while the less luminous ones are a mixture of objects with massive and less massive progenitors. Therefore, the most luminous PNe probe, on average, more recent epochs of the galaxy histories. For feasability reasons, our spectroscopic observations of PNe in M 31 and M 32 concern only objects that are luminous in [O III]. To meaningfully compare the PN abundances in these galaxies with those in the Galactic bulge and the Magellanic Clouds, we must consider samples of similar luminosities. We

[3] Table 2 is accessible only in electronic form.

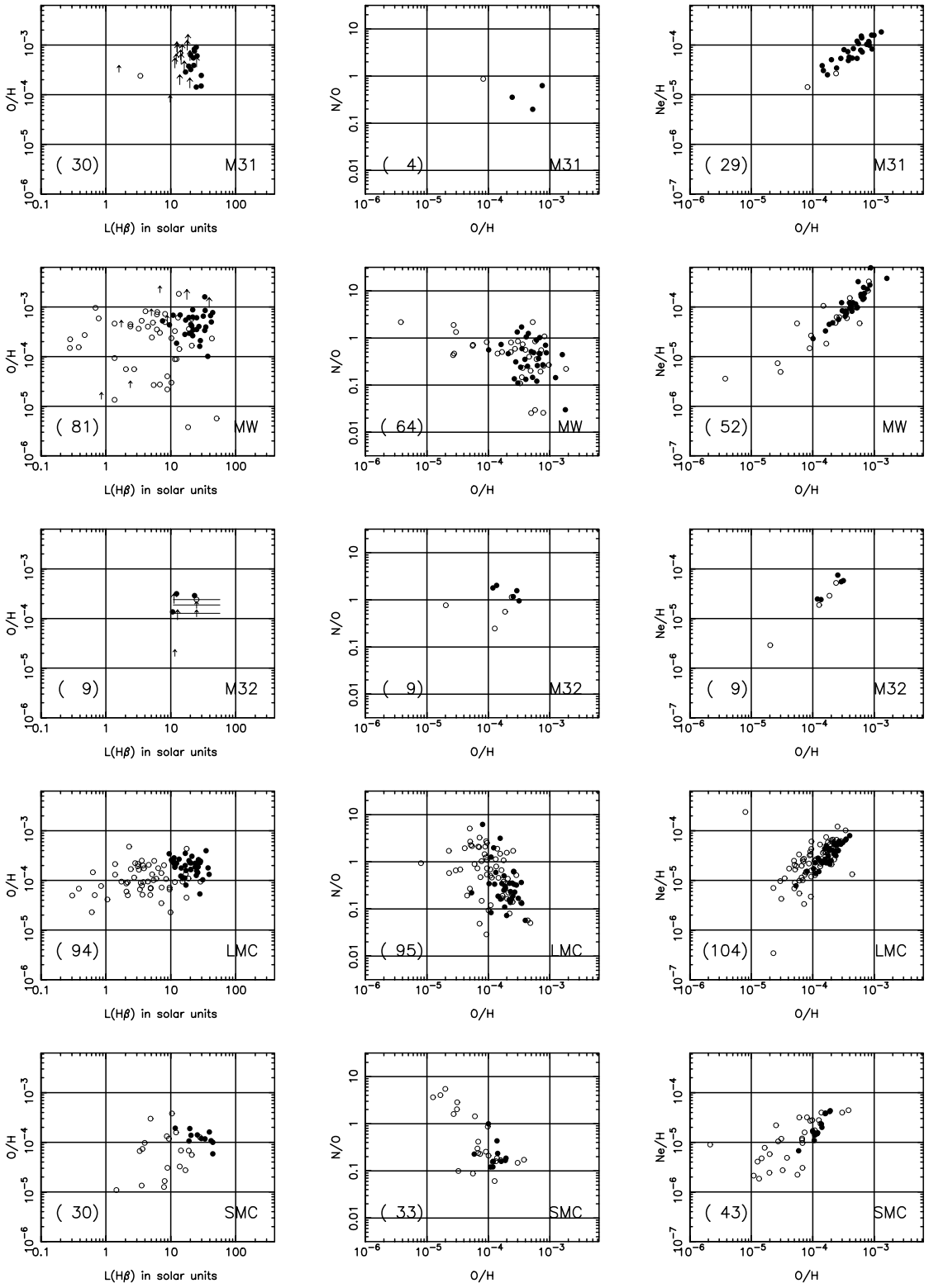

Fig. 1. PN abundance patterns in the various galaxies. Left column: O/H versus $L_{H\beta}$ in solar units. For M 32, the three PNe with unknown luminosity are represented assuming $L_{H\beta} = 25\ \mathrm{L}_\odot$, with a horizontal error bar. Middle column: N/O versus O/H. Right column: Ne/H versus O/H. Each row corresponds to a different galaxy, whose name is indicated in each panel (MW stands for Milky Way). In all the panels: PNe having $L_{[\mathrm{O\,III}]} > 100\ \mathrm{L}_\odot$ are represented by filled circles (or long arrows if only an upper limit is available for the [O III]4363 intensity), PNe having $L_{[\mathrm{O\,III}]} < 100\ \mathrm{L}_\odot$ are represented by open circles (or short arrows if only an upper limit is available for the [O III]4363 intensity). The total number of objects in each panel is indicated in parentheses.

have therefore divided the PNe into two groups: a high luminosity one ($L_{[\mathrm{O\,III}]} > 100$ L$_\odot$), comprising most of the M 31 and M 32 PNe, and a low luminosity one ($L_{[\mathrm{O\,III}]} < 100$ L$_\odot$). In the figures, the high luminosity PNe are represented by filled circles (or long arrows if only an upper limit is available for the [O III]4363 intensity, leading to a lower limit on O/H). The low luminosity ones are represented by open circles (or short arrows if only an upper limit is available for the [O III]4363 intensity).

For each galaxy, Table 3 gives the mean and average deviation of log O/H +12 and of log N/O, for the whole sample of PNe observed in each galaxy and for the high luminosity sample only. The number of objects concerned in each case is indicated in parentheses. Objects for which the abundances have been derived using an upper limit on the intensity of [O III]4363 have been included in the table, so that the true means for the oxygen abundance are probably slightly larger in the Galactic bulge and in the M 31 and M 32 samples. The fact that, in M 31 and M 32, the average of the upper limits on the electron temperature is close to the average of the electron temperatures for objects with measured [O III]4363, and that the distributions of the [O III]5007/Hβ are similar in both subsamples inclines one to think that the mean oxygen abundances reported in Table 3 are close to the true means. In the high luminosity subsample of the Galactic bulge, [O III]4363 intensities are available for all the objects except a few, so the statistics presented in Table 3 are a fair representation of the abundance distribution.

The last column of Table 3 gives the percentage of PNe having log N/O > - 0.3 (corresponding to the definition of Type I PNe by Peimbert & Torres-Peimbert 1983) among those objects for which both N and O could be derived. For the PNe in the Galactic bulge and in the SMC, when N/O was not available, it was, in most cases, because neither [O II]3727 nor [O II]7325 were measured. Therefore, it is likely that the true proportion of Type I PNe is larger than reported in Table 3 for the low luminosity samples in these galaxies. For the LMC PNe, the number of objects lacking information on O^+ is about the same as the number of objects lacking information on N^+, and this number is relatively small. Consequently, the proportions reported in Table 3 should be a fair representation of the true proportions of Type I PNe in the samples considered. In M 31, only 4 objects had [N II]6583 in the observed wavelength range, so the statistics are very poor.

3.1. Oxygen

From Fig. 1 and Table 3 we can see that the oxygen abundances are, on average, larger in the high $L_{[\mathrm{O\,III}]}$ groups in every galaxy where such a comparison is statistically meaningful (MW, LMC, SMC). Fig. 1 clearly shows that the same conclusion would be reached had we defined the groups of PNe according to the Hβ luminosity, a criterion less dependent on the oxygen abundance than the [O III] luminosity. This is consistent with the idea that luminous PNe have more massive progenitors, on average, and thus probe the latest stages of the chemical evolution of the interstellar medium as compared to low luminosity PNe, which, on average, probe earlier, less enriched stages. The fact that the average oxygen abundance in a galaxy depends on the sampled luminosity range is important to keep in mind if one wishes to compare average oxygen abundances obtained by different authors for the same galaxy.

In all the galaxies with sufficient data, we also note a wide range of oxygen abundances, spanning about one order of magnitude for the most luminous PNe, and even more if low luminosity PNe are considered as well. Chemical evolution models must aim at reproducing not only the average oxygen abundence, but also this abundance dispersion which varies from one sample to another.

We now compare the average O/H abundances in the high luminosity samples. The O/H abundance distributions are fairly similar in M 31 and in the Galactic bulge. In these two galactic systems, the oxygen abundances are, on average, higher than in the Magellanic Clouds. The case of M 32 is intermediate between the Magellanic Clouds and the bulges of M 31 and of the Galaxy.

Inferences on the chemical evolution of galaxies based on these new results on oxygen abundance distributions are presented in separate papers (Richer et al. 1998b and Mc Call et al. 1998).

3.2. Neon

Concerning neon, it has been shown by Henry (1989) that PNe follow the same linear relation between log(Ne/H) and log(O/H) independent of the host galaxy (his data concerned essentially PNe in the Milky Way, the LMC and the SMC) and that this relation is the same as the one followed by giant H II regions (Vigroux et al. 1987). The universality of this relation was interpreted as a hint that O and Ne are essentially produced by stars in the same, very narrow mass range, or that the initial mass function is spatially and temporally invariant.

Fig. 1 shows that, in each of the five galactic sites we are considering, there is a strong, linear correlation between log(Ne/H) and log(O/H) (about the same everywhere), extending the relation found by Henry (1989) and Vigroux et al. (1987) towards higher metallicities.

We note that this correlation is tighter when considering the high luminosity samples only. Actually, photoionization models show that, in low luminosity PNe, the Ne^{++} and O^{++} zones are not necessarily coextensive (either because the effective temperature of the central star is small, or because the nebulae are extended and have a low level of ionization; see Stasińska 1998) and this may affect the derived Ne/O ratios by factors of up to 3–4. Therefore, part of the scatter observed for the low luminosity PNe is probably simply due to errors in the derived Ne/O ratios.

If we consider the high luminosity samples only, the orthogonal regression line defined by the PNe from all the galaxies is $log(Ne/H) + 12 = (-2.583 \pm 0.504) + (1.221 \pm 0.060)(logO/H + 12)$. A closer examination of Fig. 1 shows that the PNe in M 31 prolongate the Ne/H versus O/H relation found for the Magellanic Clouds at lower abundances. On the other hand, the high luminosity Galactic bulge PNe define an

Table 3. PN abundance patterns.

	log O/H + 12			log N/O			Type I
whole sample							
M 31	8.636	0.233	(30)	-0.355	0.222	(4)	50.0 %
MW	8.482	0.434	(85)	-0.438	0.352	(66)	42.4 %
M 32	8.182	0.246	(9)	-0.012	0.210	(9)	88.9 %
LMC	8.099	0.250	(108)	-0.353	0.415	(95)	45.3 %
SMC	7.743	0.386	(48)	-0.455	0.438	(33)	27.3 %
high luminosity sample							
M 31	8.677	0.211	(27)	-0.453	0.167	(3)	33.3 %
MW	8.671	0.213	(32)	-0.425	0.299	(31)	35.5 %
M 32	8.315	0.169	(5)	0.161	0.109	(5)	100.0 %
LMC	8.279	0.134	(40)	-0.518	0.291	(37)	21.6 %
SMC	8.095	0.107	(11)	-0.658	0.199	(10)	10.0 %

almost perfect correlation for log O/H +12 between 8 and 9, but offset towards higher neon abundances (by about 50 %) as compared to the other galaxies. If this offset were proved to be real, it might indicate a different chemical evolution in the Galactic bulge compared to M 31.

3.3. Nitrogen

Part of the nitrogen observed in all PNe was manufactured by their precursor stars. The magnitude of this manufactured fraction depends upon the star's initial mass and metallicity, and is much larger in more massive intermediate-mass stars that undergo the second dredge-up (e.g. Forestini & Charbonnel 1997; van den Hoek & Groenewegen 1997). Commonly, it is assumed that planetary nebulae with N/O exceeding some fiducial value ($\log \mathrm{N/O} > -0.3$) are the offspring of intermediate-mass stars that underwent the second dredge-up. However, when setting this fiducial value, the precursor stars' initial nitrogen and oxygen abundances ought to be considered, particularly when comparing PNe in different galaxies. If the initial stellar N/O ratios were very different in two galaxies, it is clearly incorrect to use a single fiducial N/O ratio to ascertain whether the second dredge-up occurred in the stars that produced their PNe. In the galaxy with the initially higher N/O ratio, a smaller nitrogen production would artificially qualify its stars as second dredge-up candidates. This issue is important here, for the stellar nitrogen abundance is known to be enhanced in the nucleus of M 31, and the N/O ratio may well be a factor of 2 to 3 higher than in the Milky Way bulge (Worthey 1996).

When comparing the N/O ratios of PN populations in different galaxies, it is also important to consider the effect of the star formation history. In a galaxy with ongoing star formation, all intermediate-mass stars contribute to the production of PNe. In a galaxy where star formation stopped some time ago, the mass range of PN progenitors is considerably reduced, because the higher mass progenitors no longer exist. Since the processes that modify a star's initial nitrogen abundance depend upon its initial mass (Forestini & Charbonnel 1997; van den Hoek & Groenewegen 1997), the processes responsible for the N/O ratios observed in the PN populations in galaxies with different star formation histories could be very different.

The statistics on nitrogen from our new data on M 31 and M 32 are rather sparse, compared to the other galaxies. Still they improve over what was known before, on the account of the number of objects and quality of data. The suggestion made by Ford (1983) that the PNe in M 32 are nitrogen rich is confirmed: we find that all the luminous PNe in M 32 have N/O > 1. In the high luminosity groups of the remaining galaxies, the percentage of PNe with high N/O ($\log \mathrm{N/O} > -0.3$) ranges from 35 % in the Galactic bulge to 10 % in the SMC. It seems unlikely that all the luminous PNe in M 32 have high enough central star masses to undergo the second dredge-up, since this is not the case in the other galaxies under study (even in the ones with the most recent star-forming events). Therefore, our finding suggests that, in M 32, nitrogen was already enhanced in the precursor stars.

It has already been noted before that N/O was anticorrelated with O/H in the Magellanic Clouds and the Milky Way disk (e. g. Peimbert 1985, Leisy & Dennefeld 1996). Fig. 1 confirms this relation for the LMC and SMC on larger samples, and indicates a similar (though less prominent) relation in the Galactic bulge. One explanation commonly invoked is the effect of second dredge-up and hot bottom burning, which both deplete oxygen at the same time as they enhance nitrogen, and take place in the PNe with massive central stars. However, such a statement still requires quantitative checking. Let us simply note here that the negative oxygen yield of Forestini and Charbonnel (1997) is not likely to affect strongly the oxygen abundance. Our finding (see Fig. 1) that the largest N/O ratios occur in the low luminosity samples of PNe (if one excepts M 32) could be interpreted by saying that the PNe with the most massive central stars are those that are most likely to be seen on the descending evolutionary tracks, and thus at low luminosities, as suggested by Kaler & Jacoby (1991). However, the large number of objects observed with high N/O ratios and [O III] luminosities between 10 and 100 times solar does not support such a view, and we are inclined to think that these objects correspond, on the contrary, to smaller central star masses. Yet, following the computations of

the yields by Forestini and Charbonnel (1997), one expects the highest N/O at the largest metallicities and for the most massive stars, exactly the opposite of what can be inferred from Fig. 1. However, as emphasized by van den Hoek and Groenewegen (1997) in their Figs. 1 and 2, yields are dependent upon various free parameters in the computations, such as the mass loss rate or the dredge up efficiency, so that an ab initio prediction of the nitrogen production and a meaningful comparison with the observed PN abundances is still ahead of us.

4. An empirical comparison of the PN populations in the various galaxies

4.1. Noticeable observational facts

Because the PNe in our samples have such different oxygen abundances, we must work with observational diagrams that are not directly dependent on metallicity. The total luminosity in Hβ is a convenient parameter, which depends only weakly upon metallicity through the dependence of recombination coefficients on the electron temperature of the nebular gas. The O^{++}/O^{+} ratio is a rough description of the ionization structure of the nebula, also not too dependent on the electron temperature. The He II 4686/Hβ ratio is, above all, a strong function of the effective temperature of the ionizing star and of the proportion of stellar photons absorbed by the nebular gas. It also depends on the dilution of the PNe. Its dependence on He/H or O/H is minor.

We will thus consider 3 diagrams: He II 4686/Hβ vs. $L_{H\beta}$, O^{++}/O^{+} vs. $L_{H\beta}$ and O^{++}/O^{+} vs. He II 4686/Hβ, represented in the left, middle, and right panels of Fig. 2, respectively. Fig. 2 is otherwise organized in a similar way to Fig. 1, and the symbols have the same meaning, except that, in panels involving O^{++}/O^{+}, objects with only an upper limit available for both [O III]4363 and [O II]3727 are represented with a + sign. Actually, the error on O^{++}/O^{+} due to the lack of an electron temperature measurement is rather small (less than 50 %), so that, in most cases, the real significance of a + sign is probably a lower limit to O^{++}/O^{+}.

In these diagrams, the PN populations in the different galaxies look strikingly different. If we consider only the high luminosity PNe, we see that, in the Magellanic Clouds, *all* the measured He II 4686 /Hβ ratios but one are greater than 0.1. Objects where He II 4686 has not been measured are not expected to fill this gap, since in many of them, other low intensity features, such as [O III]4363, have been measured down to intensities about 0.01 of Hβ. On the other hand, in the Galactic bulge, half of the high luminosity PNe with measured He II 4686 have He II 4686/H$\beta < 0.1$, and in M 31 the proportion is two thirds. For M 32, the statistics are poorer, but the trend looks similar to that of the Magellanic Clouds.

In the O^{++}/O^{+} versus $L_{H\beta}$ diagram, the high luminosity PNe in the Galactic bulge lie, on average, higher than their counterparts in the LMC. In M 31, the O^{++}/O^{+} ratios are, on average, much higher than elsewhere, and all have $O^{++}/O^{+} > 10$. Before accepting such a result, we examined the reasons that might bias the derived O^{++}/O^{+} ratios in M 31. Since all the PNe in M 31 show relatively weak [O II]3727, we wondered if something might be amiss with the instrumental calibration of that data. However, as shown in Richer et al. (1998a), both internal and external consistency checks indicate that the instrumental calibration is not in error, particularly in the blue. The observed reddening for the PNe in the bulge of M 31 is modest (see Sect. 2.1), so it seems unlikely that their [O II]3727 intensities could seriously be in error on account of the reddening. A systematic overestimation of the electron temperature in the O^{+} zone, such as might be expected if the N/O ratios in the bulge of M 31 were significantly higher than elsewhere, would have to be of about 2 000 K in order to produce an overestimation of O^{++}/O^{+} by a factor 2. We checked by running various photoionization models, that the temperatures in the O^{++} and O^{+} zones in high excitation PNe are always very similar, regardless of the abundance ratios. Another possibility would be to put the blame on [O III]5007. Indeed, we note that in our M 31 PNe, the [O III]4363/Hβ ratios are high compared to the other galaxies. For PN29, which we have in common with Jacoby (private communication), we estimate an [O III]4363/Hβ of 22, while Jacoby finds 15 (the other lines being in reasonable agreement). We reconsidered our data very carefully, and could not come up with a good explanation for this discrepancy. The only reasonable hypothesis would be a different correction for background Hβ which, in both cases, is done by examining the spatial variation of Hβ along the slit. We note however that, if our Hβ intensity were underestimated, this would not alter the O^{++}/O^{+} ratios, but would instead affect all the line ratios with respect to Hβ. Then, the He II 4686/Hβ we give would be overestimated, making the difference with the Magellanic Clouds even more conspicuous. In the following, we adopt the view that our line intensities are correct, keeping in mind that this matter deserves more thorough observational investigation.

Finally, we note from the O^{++}/O^{+} versus He II 4686/Hβ diagram, that, in M 31, many PNe with high O^{++}/O^{+} show, unexpectedly, a low He II 4686/Hβ.

In summary, the PN systems show very different behaviours in the diagrams of Fig. 2. The most striking differences are found between our M 31 PNe sample and the [O III]-bright PNe in the LMC. Briefly, the M 31 PNe are characterized by large O^{++}/O^{+} ratios (about 10–100), and modest He II 4686/Hβ ratios (0.1–0.2, when above detection threshold), while the LMC ones are characterized by smaller O^{++}/O^{+} ratios (0.3–30) and high He II 4686/Hβ ratios (0.2–0.8). Such differences undoubtedly indicate that the [O III]-bright PN populations are not the same in these galaxies.

4.2. A naive interpretation

The fact that the He II 4686/Hβ ratios are, on average, larger in the Magellanic Clouds than in the Galactic bulge or in M 31 could suggest, at first sight, that the effective temperatures are larger. This, in turn, could be understood as an indication that the same ranking holds for the masses of the central stars, $M_\star$, using the common argument (e.g. Webster 1988) that, during

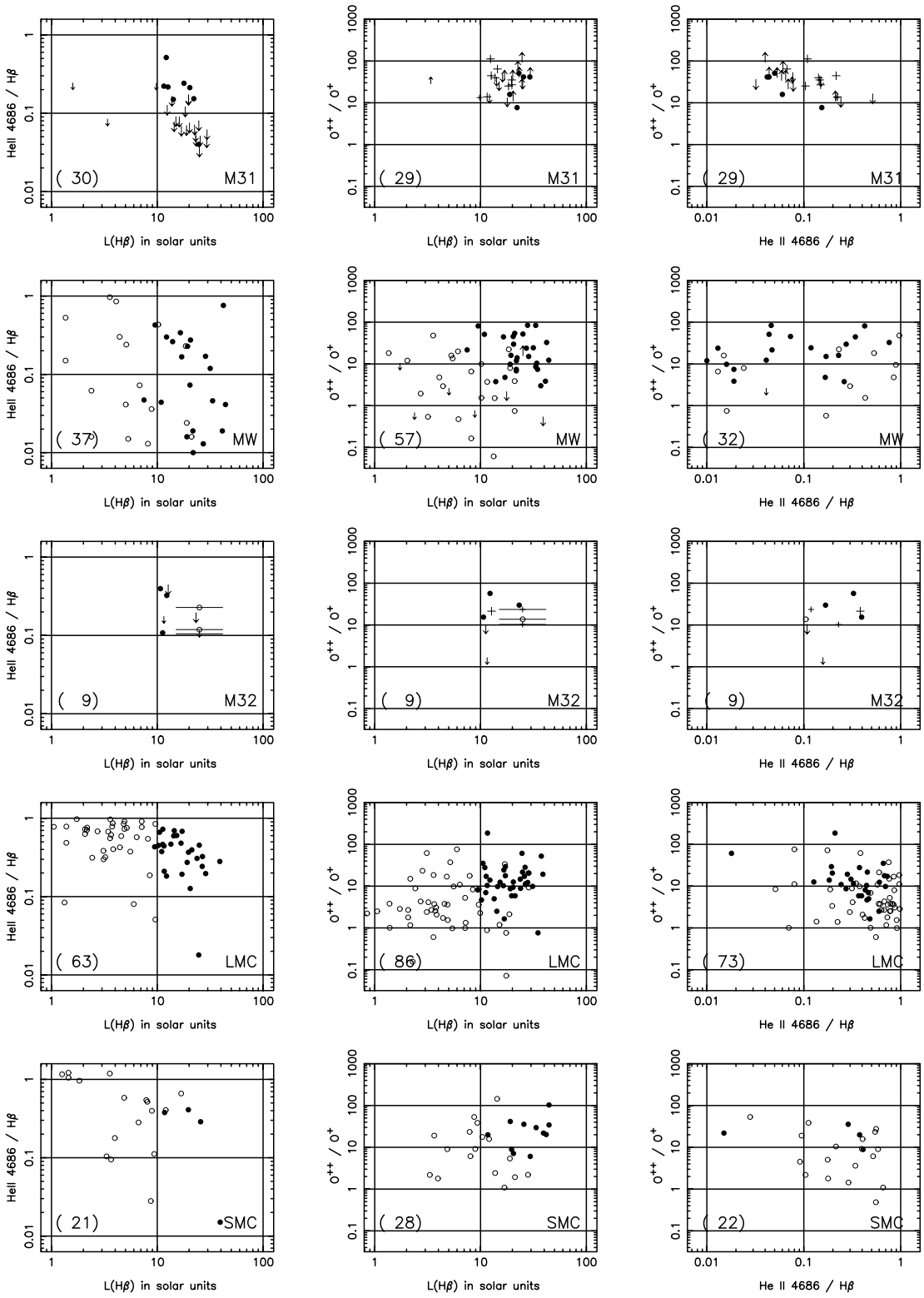

Fig. 2. PN excitation diagrams in the various galaxies. Left column: He II 4686/Hβ versus $L_{H\beta}$. Middle column: O^{++}/O^{+} versus $L_{H\beta}$, right column: O^{++}/O^{+}versus He II 4686/Hβ. Each row corresponds to a different galaxy, whose name is indicated in each panel (MW stands for Milky Way). Symbols have the same meaning as in Fig. 1, except that arrows represent limits on He II 4686/Hβ (left column) or O^{++}/O^{+} (middle and right columns). Objects where only an upper limit is available for both [O III]4363 and [O II]3727 are represented with a + sign.

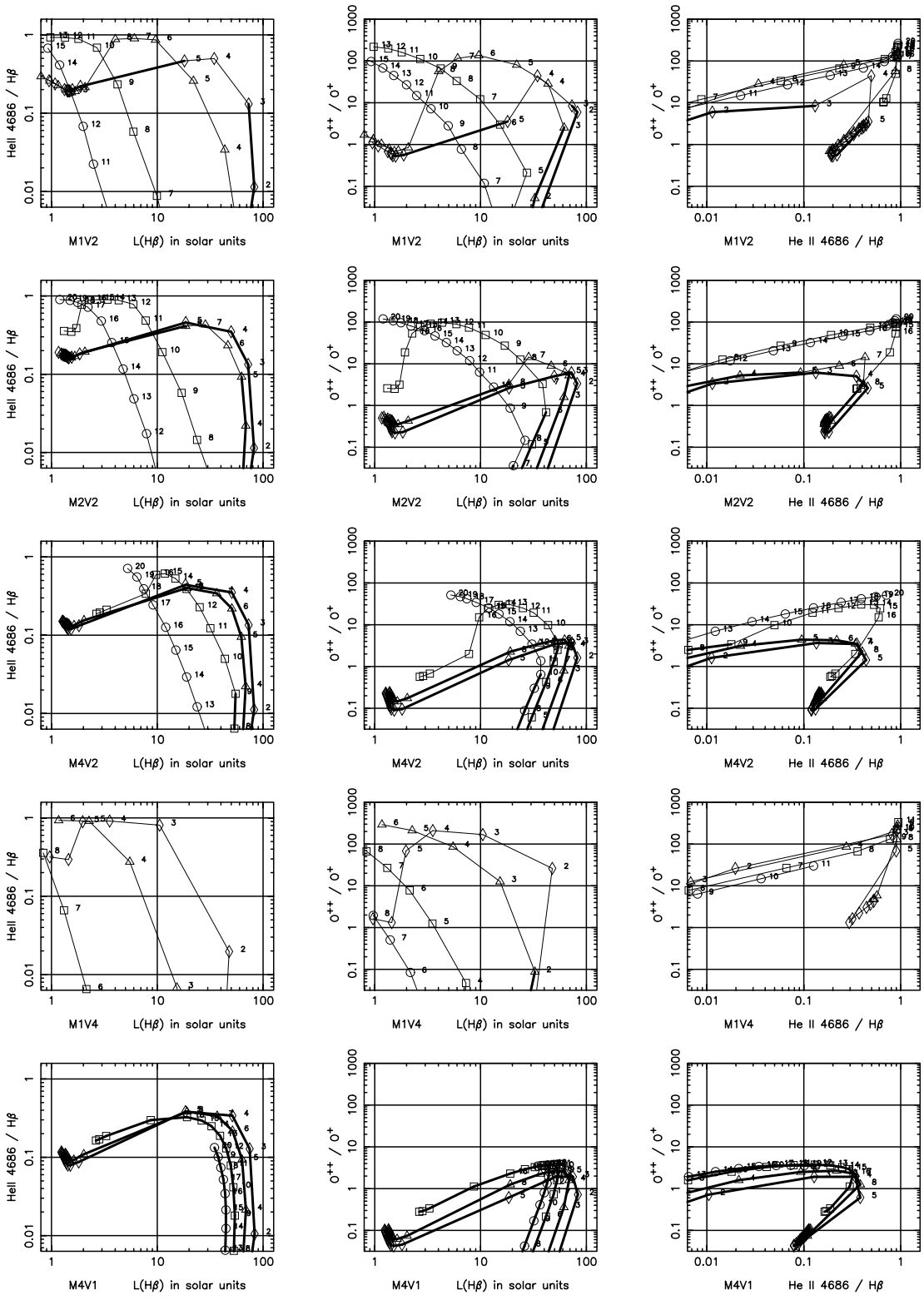

Fig. 3. Evolutionary tracks of models of PNe in the same coordinates as Fig. 2. The various rows correspond to different combinations (see text) of the assumed nebular mass, M_{neb}, and expansion velocity, v_{exp}, as indicated below each panel. The different tracks correspond to different central star masses, $M_\star$. At each time step of 500 yr, until an age of 10 000 yr is reached, the tracks are marked by a symbol, whose label represents the age in units of 500 yr (in order to avoid crowding, the label appears only while the star is on its heating track). Different values of $M_\star$ are represented by different symbols: 0.58 $M_\odot$ (circles), 0.60 $M_\odot$ (squares), 0.62 $M_\odot$ (triangles), 0.64 $M_\odot$ (diamonds). Thick lines: optically thick stages; thin lines: optically thin stages.

their evolution, higher mass central stars reach higher effective temperatures. However, as will be seen in the next section, such an argument is not correct.

One would expect high He II 4686/Hβ ratios to be associated with high O^{++}/O^{+} ratios. Yet, as stated above, this is not what is observed, since the samples with higher O^{++}/O^{+} (M 31) and the samples with higher He II 4686/Hβ (LMC, SMC) are not the same. One explanation could be that the Magellanic Clouds PNe are more clumpy than those in M 31, so that their low excitation lines are enhanced. It is more difficult to understand why, in M 31, we see PNe with a high O^{++}/O^{+} and a low He II 4686/Hβ. We shall come back to this in Sect. 6.

5. Theoretical evolution of planetary nebulae

In principle, one can do better than just a naive interpretation. Indeed, theoretical evolutionary tracks for PN central stars are available (e.g. recently Blöcker 1995, Vassiliadis & Wood 1994) and can be coupled to photoionization models of PNe. Once the properties of the central star and of the nebula have been specified, one can then predict the intensities in the various emission lines. What one would like, with such models, is to understand what drives the differences observed among the PN populations in the various galaxies.

5.1. The model grid

We use the set of hydrogen burning post-AGB evolutionary tracks of Blöcker (1995, and references therein), with the same interpolation procedure as in Stasińska et al. (1997). The stars are assumed to radiate like blackbodies, and ionize the surrounding nebular envelopes, assumed spherical. There are at least two parameters that define the photometric and spectroscopic appearance of a PN surrounding a star of given mass at a given epoch. These are the total nebular mass, M_{neb} (which includes both the ionized and neutral component), and the nebular expansion velocity, v_{exp}. We consider uniformly expanding nebular shells of constant relative thickness $\Delta R/R$ = 0.3, in which the density, assumed uniform, is varied with time appropriately.

These models are deliberately simple. They correspond to a naive representation of the nebular evolution (actually, this is precisely the representation one has in mind when expressing qualitative arguments on PN evolution) and they must be considered as an anchor point for more elaborate considerations. Their main virtue is that, within the specified properties of the central stars and surrounding nebulae, they are accurate, and allow a meaningful comparison with the observations. By using them, as a first approximation, one can then try guessing what happens if the nebular geometry and evolution are different from the ones assumed in the models.

Another approach, used by Dopita & Meatheringham (1991) for the Magellanic Clouds PNe, is to derive the stellar temperatures and luminosities by computing photoionization models fitting the observed emission line intensities (essentially, in the case of Dopita & Meatheringham, He II 4686/Hβ, when observed, [O III]5007/Hβ and $L_{H\beta}$, all of these with a rather large tolerance), and then place the objects in an HR diagram. The advantage of such a method is that it does not assume anything a priori about nebular or stellar evolution. However, it is difficult to apply for large samples like the ones we are considering. Our method has also the advantage of a greater pedagogical value and an easy extension to other samples of PNe.

Fig. 3 gives the results obtained for a few series of models which roughly span the range of parameters one expects to be relevant to PN studies [4]. The three panels in each row have the same coordinates as those of Fig. 2, so that comparison with the location of observational points is straightforward by superposition. The different rows in Fig. 3 correspond to different combinations of the assumed M_{neb} and v_{exp}. The first row corresponds to a nebular mass $M_{neb} = 0.1$ $M_\odot$ and an expansion velocity $v_{exp} = 20$ km s^{-1} (label: M1V2 on the horizontal axis). The 2nd row corresponds to $M_{neb} = 0.2$ $M_\odot$ and $v_{exp} = 20$ km s^{-1} (label M2V2). The 3rd row corresponds to $M_{neb} = 0.4$ $M_\odot$ and $v_{exp} = 20$ km s^{-1} (label M4V2). The 4th row corresponds to $M_{neb} = 0.1$ $M_\odot$ and $v_{exp} = 40$ km s^{-1} (label M1V4), and the 5th row to $M_{neb} = 0.4$ $M_\odot$ and $v_{exp} = 10$ km s^{-1} (label M4V1). The different tracks correspond to different central star masses, $M_\star$. At each time step of 500 yr, until an age of 10 000 yr is reached, the tracks are marked by a symbol. The label beside it represents the age in units of 500 yr (in order to avoid crowding, the label appears only while the star is still on its heating track). Different values of $M_\star$ are represented by different symbols: 0.58 $M_\odot$ (circles), 0.60 $M_\odot$ (squares), 0.62 $M_\odot$ (triangles), 0.64 $M_\odot$ (diamonds). The portions of the tracks where the ionized mass is equal to the total nebular mass (the nebula is "density bounded" or "optically thin") are drawn with a thin line.

5.2. A few remarks about the model results

The general appearance of the theoretical evolutionary tracks of our model PNe depends strongly upon both the nebular mass and the expansion velocity. It is straightforward to show that, when a PN is optically thin (and still with a high degree of ionization), its Hβ luminosity, at a given epoch, is proportional to M_{neb}^2/v_{exp}^3 and is independent of the central star properties, while the O^{++}/O^{+} ratio, linked to the ionization parameter, goes roughly like v_{exp}/M_{neb}. The He II 4686/Hβ ratio is proportional to v_{exp}^3/M_{neb}^2 if the nebula absorbs all the He^{+} ionizing photons. When a PN is optically thick, the Hβ luminosity and He II 4686/Hβ ratios obviously depend only on the characteristics of the central star, while O^{++}/O^{+} depends also on the characteristics of the nebula, M_{neb} and v_{exp}. In a PN of

[4] Detailed results of the whole grid of models considered in the present study, including the intensities of about 100 lines and various other useful quantities, can be retrieved by anonymous ftp from cdsarc.u-strasbg.fr (130.79.128.5). The models presented in Fig. 3 of this paper correspond only to a selection of the whole grid. We have also computed models with lower and higher central star masses, up to 0.90 $M_\odot$, and with O/H ratios of $8.5\,10^{-5}$ and $1.7\,10^{-3}$, in addition to the ones with O/H = $4.2\,10^{-4}$ shown in Fig. 3. The discussion presented below takes into account those models as well.

given central star mass, the transition time from the optically thick to the optically thin regime occurs at a time that goes like $M_{neb}^{(2/3)}/v_{exp}$. Knowing these simple rules, one can roughly interpolate between the five series of models presented in Fig. 3 to span the whole range of PN properties a priori expected for $M_\star$ between 0.58 and 0.64 $M_\odot$.

If we now examine Fig. 3, we see that, for $M_{neb} = 0.1$ $M_\odot$ and $v_{exp} = 40$ km s^{-1}, all the PNe with 0.58 $M_\odot < M_\star <$ 0.64 $M_\odot$ are density bounded, while for $M_{neb} = 0.4$ $M_\odot$ and v_{exp} = 10 km s^{-1}, they are all ionization bounded. For intermediate cases, schematically, PNe with central star masses of 0.62–0.64 $M_\odot$ are rather ionization bounded in the luminosity range we are interested in, while those with central star masses of 0.58–0.60 $M_\odot$ are rather density bounded.

Concerning the behaviour of the He II 4686/Hβ ratios, our models show that the highest He II 4686/Hβ ratios are not obtained for the highest $M_\star$, and correspond to rather low Hβ luminosities. They always occur when the nebulae are optically thin, and therefore are not a mere indication of the stellar temperature. It is only in high luminosity subsamples that higher He II 4686/Hβ might be indicative of a higher central star mass (see Sect. 4.2), but not necessarily.

In all our models, we find that the O^{++}/O^+ ratio roughly follows He II 4686/Hβ. Only the amplitude of its variations is larger, since one can have situations where O^+ is only a trace ion.

The variations of $L_{[O\,III]}$ as a function of time are shown in Fig. 4, for models with stellar masses of 0.58, 0.60, 0.62 and 0.64 $M_\odot$. Each row corresponds to a different combination of M_{neb} and v_{exp} (the same as in Fig. 3). As in Fig. 3, the symbols mark time steps at intervals of 500 yr. In order to easily link the variations of $L_{[O\,III]}$ with the stellar properties, we show, in Figs. 5 and 6, the variations of the stellar effective temperature, $T_\star$, and luminosity, $L_\star$, as a function of time, for the same values of $M_\star$ as in Fig. 4.

Fig. 4 shows that the maximum value of $L_{[O\,III]}$ attained during the evolution of a model PN is larger for greater $M_\star$. When the PNe are still optically thick at maximum, this is because the maximum number of ionizing photons emitted by a star is larger for greater $M_\star$. When they are optically thin at maximum, this is because the value of $T_\star$ attained at this maximum is larger. As is known, $L_{[O\,III]}$ is not strongly dependent upon the metallicity in PNe. In Fig. 4, for the M2V2 cases, in addition to models with half solar metallicity (circles), we have also plotted models with a metallicity of one tenth solar (triangles) and twice solar (squares). We see that the change in $L_{[O\,III]}$ with respect to metallicity is rather small (and not monotonic). From the above, we can say that a sample of PNe with $L_{[O\,III]}$ $>$ 100 $L_\odot$ is likely to contain PNe with more massive central stars ($M_\star = 0.60$–0.62 $M_\odot$) than a sample of PNe with 10 $L_\odot$ $< L_{[O\,III]} <$ 100 $L_\odot$ (unless the PNe have large M_{neb} and small v_{exp}, like the M4V1 models which, obviously, cannot apply to the bulk of the PNe studied here).

Fig. 4 also shows that the age range during which PNe can be seen in a distant galaxy strongly depends on the interval of luminosities that is spanned. It also depends on the central star masses, and on the nebular parameters (M_{neb} and v_{exp}). Of course, as is known, PNe with central stars with mass $\simeq$ 0.65 $M_\odot$ have very little chance of being observed at [O III] luminosities above 10 $L_\odot$, because the luminosity drop occurs very early in the central star evolution.

Not much attention has been paid so far to the behaviour of PNe when the stellar luminosity has dropped to a level which does not ensure full ionization of the gas. Such a situation is predicted by stellar evolutionary models to occur for stars with mass 0.62 $M_\odot$ and higher. After this important stellar luminosity drop, $L_{H\beta}$ is expected to vary more slowly with time than if the gas were fully ionized. The O^{++}/O^+ ratio, after having dropped because of the sudden decrease in the ionization parameter, remains more or less stationary. The He II 4686/Hβ ratio also first decreases, because a larger proportion of neutral hydrogen in the nebula competes with He^+ in the absorption of photons above 54.4eV, then becomes stationary. This produces a clump in the He II 4686/Hβ versus $L_{H\beta}$ and O^{++}/O^+ versus $L_{H\beta}$ diagrams, as seen in Fig. 3. Trying to detect such a clump requires measuring the appropriate emission lines in a complete sample of PNe down to a factor 100 below the maximum luminosity. This is a goal that can be achieved by present day equipment for the Magellanic Clouds. The detection of such a clump would be an interesting test of post-AGB evolution models. Then, knowing what proportion of low luminosity PNe are in the clump would allow one to estimate the proportion of PNe with massive central stars, and thus, the PN production rate from different stellar populations.

6. Examination of the PN populations in the light of the model grid

Confrontation of the available observations with PN evolutionary tracks is difficult, because we expect some dispersion not only in the central star masses, but also in the expansion velocities and in the nebular masses. Also, there are indications that the average nebular properties vary according to the parent galaxy. Indeed, the distribution of expansion velocities of Galactic PNe as shown in the Strasbourg-ESO catalogue (Acker et al. 1992) has a dispersion of about 10 km s^{-1} around a mean of about 20 km s^{-1} (but there are almost no data specific to the Galactic bulge). Among the Magellanic Clouds PNe, the dispersion is the same, but the mean is $\sim$ 30 km s^{-1} (Dopita et al., 1988). The range in M_{neb} is more difficult to estimate, because nebular masses are poorly known and the available data generally correspond only to the ionized part of the nebulae. It seems that in the Magellanic Clouds, the average nebular mass is about 0.3 $M_\odot$ (Barlow 1987), while in the Galactic bulge PNe, it is probably 0.1–0.2 $M_\odot$ (Stasińska & Tylenda 1994) and a dispersion of a factor two among the PNe in a given galaxy is certainly not unreasonable. Another point to consider is the following. From imaging of PNe in the Galaxy and the Magellanic Clouds, we know of many objects in which the covering factor of the matter contributing most to the luminosity is smaller than one. Thus, in order to compare a sample of observed PNe with our models,

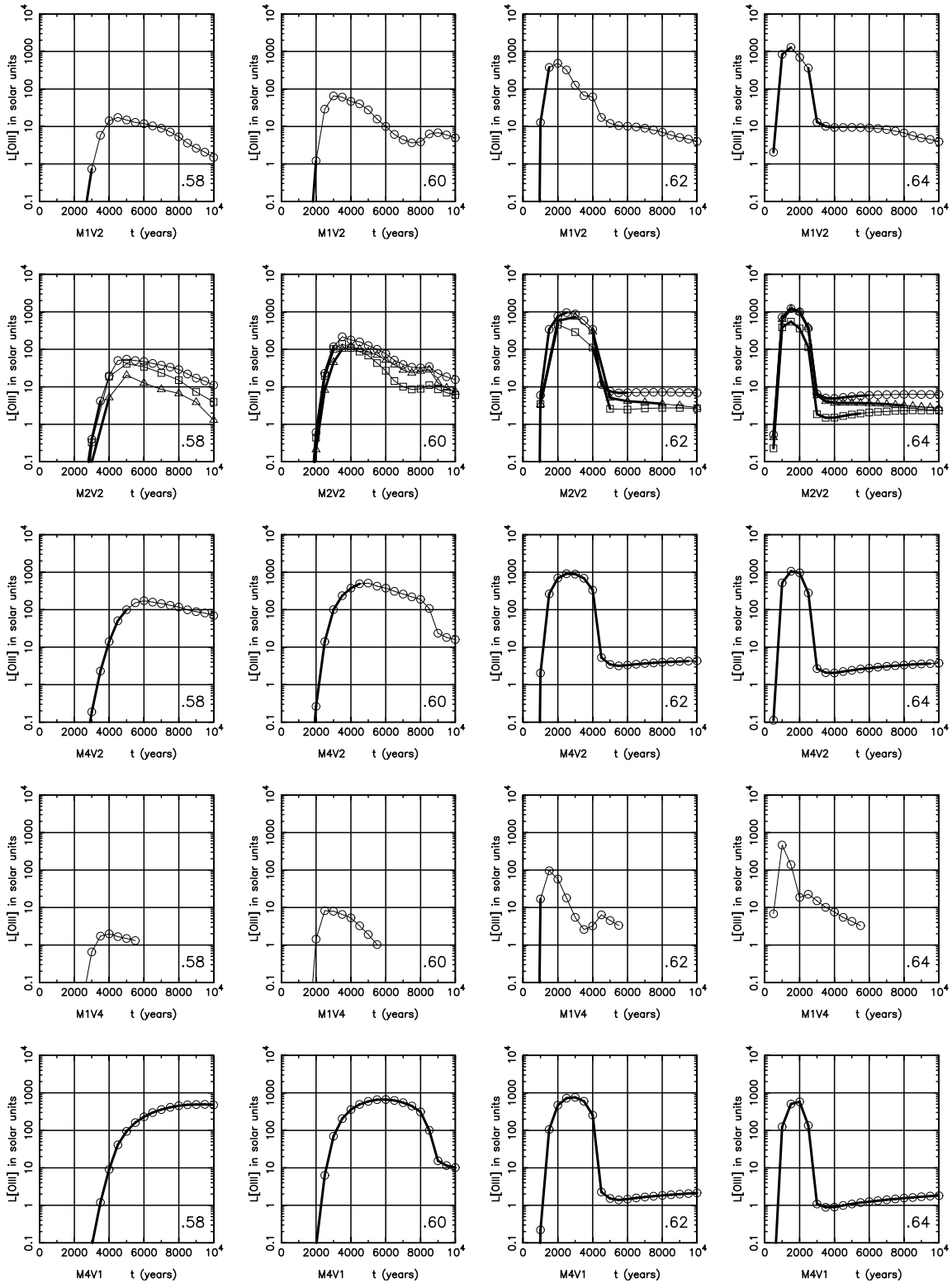

Fig. 4. Variations of $L_{[\mathrm{O\,III}]}$ (in solar units) as a function of time, for PN models with central star masses of 0.58, 0.60, 0.62 and 0.64 $M_{\odot}$. The central stars evolve according to the evolutionary tracks of Blöcker (1995). Each row correspond to a different combination of M_{neb} and v_{exp}, indicated at the bottom of each panel (the same as in Fig. 3). All the models are for half solar metallicity, except for the M2V2 cases, where we also plot models with a metallicity of one tenth solar (triangles) and twice solar (squares). As in Fig. 3, the symbols mark time steps at intervals of 500 yr. Thick lines: optically thick stages; thin lines: optically thin stages.

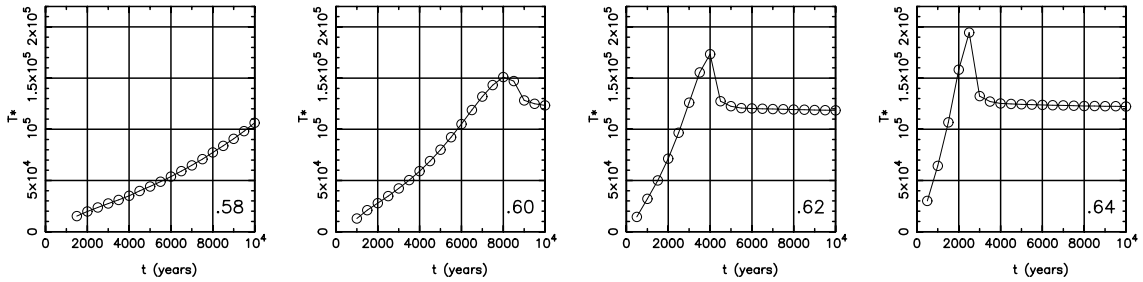

Fig. 5. Variations of the effective temperature, $T_\star$ (in Kelvin), as a function of time, for central star models of Blöcker (1995) with masses 0.58, 0.60, 0.62 and 0.64 $M_\odot$ (as indicated in each panel). The symbols mark time steps at intervals of 500 yr.

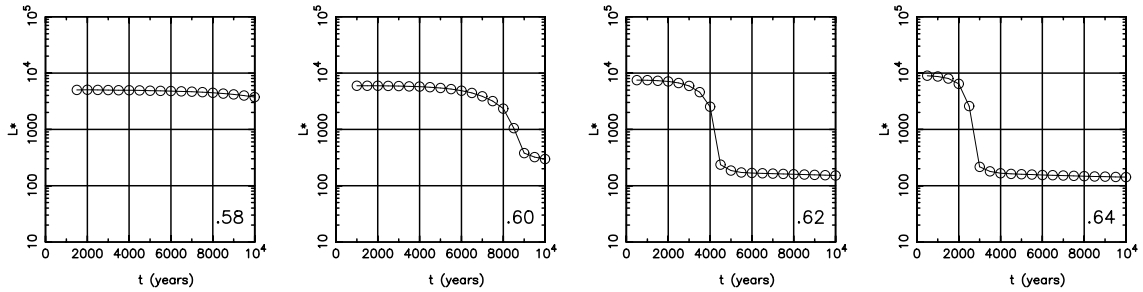

Fig. 6. Variations of the stellar luminosity, $L_\star$ (in solar units), as a function of time, for the same central star models as in Fig. 5. The symbols mark time steps at intervals of 500 yr.

one should not forget that the models might have to be shifted leftwards in Fig. 3 (perhaps by a factor 2–5).

Considering now the observational diagrams of Fig. 2 with the help of the models shown in Fig. 3, we see that the different behaviours of the PN populations in the different galaxies cannot be only attributed to a different distribution in central star masses, nebular masses or expansion velocities.

The observed positions of the Galactic bulge PNe in Fig. 2 are compatible with the computed tracks for central star masses between 0.60 and 0.62 $M_\odot$ for the high luminosity sample, and between 0.58 and 0.60 $M_\odot$ for the low luminosity sample, if one assumes a typical M_{neb} of 0.2 $M_\odot$ and a typical v_{exp} of 20 km s^{-1}. Of course, the central star mass estimate would be shifted towards higher values if lower nebular masses or higher expansion velocities were more appropriate.

If we now turn to the Magellanic Clouds PNe, from what we know about the expansion velocities and nebular masses, the M2V2 series should best represent the average trend observed in Fig. 2 (but the other series must not be discarded, because a dispersion in the nebular properties is expected). We immediately see that the distribution of He II 4686/Hβ ratios in the models (roughly as many symbols in the 0.01 $<$ He II 4686/Hβ $<$ 0.1 range as in the He II 4686/Hβ $>$ 0.1 range for $L_{H\beta}$ $>$10 $L_\odot$) is in conflict with the observed distributions. We are thus led to conclude that the central stars in the Magellanic Clouds do not evolve as predicted by the models of Blöcker (1995). They must evolve more rapidly during the phase where the effective temperature increases. This is surprising since the evolutionary time of post-AGB stars on the horizontal part of the HR diagram depends on the mass-loss rate in the sense that it is shorter for higher mass loss rates (see e.g. Górny et al. 1994). If mass-loss rates are smaller at lower metallicities, then one would expect a longer evolution time during the horizontal phase for the central stars of the PNe in the Magellanic Clouds as compared with Galactic bulge PNe. At this point, it is interesting to recall the works of Vassiliadis & Wood (1994) and of Dopita et al. (1997). These authors concluded that hydrogen burning models for the central star evolution spend too short a time in the ($L_\star$, $T_\star$) region where Magellanic Clouds PNe are seen. They argued that helium burning models, which spend a long time during their evolution in the high $L_\star$, high $T_\star$ zone, were more appropriate for about half of their objects.

As regards the M 31 sample, it is more difficult to analyze, since nothing is known about the PN expansion velocities or nebular masses there. Still, some interesting remarks can be made. The distribution of the observed He II 4686/Hβ ratios as a function of $L_{H\beta}$ defines a central star mass range much narrower than in the Magellanic Clouds and in the Galactic bulge (in the same [O III] luminosity interval). Indeed, the Hβ luminosity range in which He II 4686/Hβ is observed to be larger than 0.1 is very restricted in M 31. However, one must recall than the Galactic bulge sample was defined by the condition that the PN radio flux at 6 cm should be smaller than 100 mJy, and a priori, we do not know what is the maximum luminosity of the PNe in the Galactic bulge. From the histogram of the fluxes of PNe seen in the direction of the Galactic bulge (Stasińska & Tylenda 1994), this upper limit could perhaps be lowered by 20 %, but not significantly more. Thus, it seems that the mass distribution of the central stars of [O III]-bright PNe is indeed narrower in M 31 than in the Galactic bulge.

We note that, especially in M 31, the observed range in $M_\star$ is smaller than that imposed by the natural selection effect that

PN central stars necessarily have masses between 0.555 $M_\odot$ and about 0.7 $M_\odot$ in order to be seen in our samples.

The observed O^{++}/O^+ ratios bear some light on the density distribution of the nebular envelopes. In the Magellanic Clouds, the modest O^{++}/O^+ ratios that are observed while the He II 4686/Hβ ratios are large could indicate that the nebulae are optically thick. A similar behaviour would however be obtained for models that are optically thin, but with a clumpy structure. In M 31, the large observed O^{++}/O^+ ratios for objects with modest He II 4686/Hβ can be explained by an outward decreasing nebular density distribution, which would enhance the O^{++}/O^+ ratio with respect to He II 4686/Hβ as compared to a constant density shell. Another option is that the nebulae are already optically thin while the central stars are still moderately hot. This can be achieved with rapidly expanding PN envelopes, yet with a nebular mass large enough (since we are concerned with bright PNe): this, in turn, requires the stellar luminosities to be rather large and implies a different stellar evolution than assumed in our models.

In summary, we arrive at the conclusion that, probably, both the stars and the nebulae are different in the high luminosity PN samples of the different galaxies under study. It is most likely that this conclusion would remain valid had we adopted a different, perhaps more physical, evolutionary model for the nebulae.

That the PN populations the galaxies we studied are intrinsically different is not surprising, given that the star formation histories are not the same, so that the progenitors are expected to differ both in composition and in mass range.

Finally, we note that, if, in M 31, the bright PNe effectively have the high O^{++}/O^+ ratios indicated by our observations, then they must be optically thin. If so, the PN luminosity function in M 31 is only weakly dependent on the stellar properties. Interestingly, Ciardullo (1995) and Richer et al. (1997) had precisely found that the observed PN luminosity function in M 31 could be reproduced with optically thin nebulae.

7. Conclusion

We have collected photometric and spectroscopic data on PNe in 5 different galactic contexts: two samples concern bulges of spiral galaxies (M 31 and the Milky Way), one concerns an elliptical galaxy (M 32), and two concern irregular galaxies (the LMC and the SMC). Since the star formation histories of these galaxies are different, one expects their PN populations to differ. This is indeed what our analysis reveals, in spite of the fact that all these galaxies have a similar upper PN luminosity function.

We have computed the abundances of O, Ne and N in all the PNe and analyzed the abundance patterns observed in the various galaxies, separating the PNe into high luminosity (LO III $>$ 100 $L_\odot$) and low luminosity subsamples. We showed that our high luminosity samples are likely to contain a larger proportion of PNe with rather massive central stars ($M_\star$ about 0.60–0.62 $M_\odot$), while our low luminosity ones should rather contain PNe with $M_\star$ about 0.58–0.60 $M_\odot$, so that the high luminosity samples probe the interstellar medium at more recent times than the low luminosity samples. We find that the mean O/H ratio is larger for the high luminosity samples, in agreement with the idea of a gradual enrichment of the interstellar medium in oxygen. Also, the mean O/H is larger in the bulges of spirals than in the irregulars. Inferences on the chemical evolution of galaxies based on these oxygen abundances are examined in two companion papers (Richer et al. 1998b and Mc Call et al. 1998).

Concerning neon, we find that, in all the galaxies, PNe (especially the most luminous ones, where the neon abundances are believed to be more accurate) define the same linear relation between log (Ne/H) and (O/H). This extends to higher abundances the result which was already known for PNe in the Magellanic Clouds, the Galactic disk and for H II regions in irregular and blue compact galaxies. The fact that this relation holds over such a wide range of abundances favours the hypothesis that neon and oxygen are produced in the same stars. We note, however, that in the Galactic bulge, this relation seems slightly offset towards higher Ne abundances.

N/O ratios in PNe are not easy to interpret, since part of the nitrogen was produced by the progenitor stars and brought up to the surface by successive dredge-up events. In addition, when comparing the N/O ratios in PNe in different galaxies, one should consider that the N/O ratios at the time when the progenitors were born may have been different, due to a different chemical evolution and star formation histories of the parent galaxies. Nevertheless, we observe the highest N/O ratios at the smallest metallicities and at the smallest luminosities, which is puzzling, considering what is known about evolution of intermediate-mass stars. It is only in M 32, where the data are scarce, that such an anticorrelation is not seen. In this galaxy, all the observed PNe are nitrogen rich, and all the high luminosity ones have N/O > 1, which seems to indicate that the stellar nitrogen abundance is enhanced.

We have also compared the PN evolution in our 5 galaxies by constructing diagrams that are independent of abundances, and have found strongly different behaviours of the various high luminosity samples. The largest differences are found between the samples in the Magellanic Clouds and M 31: the former show high He II 4686/Hβ ratios and modest O^{++}/O^+ ratios, the latter has modest He II 4686/Hβ ratios and high O^{++}/O^+ ratios.

In order to interpret these differences in terms of central star and nebular envelope properties, we have constructed a grid of PN photoionization models in which the stellar evolution is interpolated from the Blöcker (1995) tracks, and in which the evolution of the PN envelopes is treated in a simple manner. These models demonstrate the influence of such parameters like the nebular mass or the expansion velocity on the spectroscopic signatures of the PN evolution and on the PN luminosity function. Also, they can serve as anchor points to interpret observational data on PN populations, keeping in mind that the true PN evolution might be somewhat different from what is assumed in the models. All the models that have been constructed for this project are accessible by anonymous ftp as explained in Sect. 5.1.

We found that the observational diagrams of the PNe in the Galactic bulge are roughly consistent with our evolutionary models of PNe. It seems that, in M 31, the central star mass range is narrower than in the Galactic bulge. Perhaps the reason is that the Galactic bulge sample actually contains a non-negligible proportion of disk objects. The exact value of the central star mass range, though, cannot be specified, because its determination requires a knowledge of the typical nebular masses and expansion velocities, which are presently unknown. There is some indication (which needs confirmation) that, in M 31, the central stars might evolve differently from the considered models. We note that, in this galaxy, the PN luminosities are only weakly dependent on the stellar properties, since most PNe are probably optically thin.

In the Magellanic Clouds, we do have information on both the nebular masses and expansion velocities. But the comparison of the observational diagnostic diagrams with our grid of photoionization models indicates that the hydrogen burning stellar evolutionary models of Blöcker (1995) fail in describing the evolution of PN central stars in these galaxies: the timescale for the effective temperature rise is too long. Thus, the central star evolution is not the same in the Magellanic Clouds and in the bulges of spirals.

We also find, from an examination of the behaviour of the O^{++}/O^{+} ratios, that the structure of the nebular envelopes is different in the PNe of the various galaxies under study. This indicates that the mass ejection process and the subsequent dynamical evolution of the PNe should be different.

To summarize, we find that the PN populations are not the same in the various parent galaxies. Both stars and nebulae are different. Additional observational data (especially measurement of PN expansion velocities in the Galactic bulge, M 31 and M 32, and high quality spectroscopy of PNe in M 31) would help in the characterization of these populations.

Finally, we have shown that a similar set of data on complete samples of PNe at fainter luminosities (down to about a factor 100 below the maximum) would make it possible to directly estimate the proportion of PNe with high mass ($M_\star \geq 0.62$ $M_\odot$) central stars in a given population.

Acknowledgements. We thank G. Jacoby who, through a thorough refereeing of this paper, raised several interesting (yet unsolved) questions.

References

Acker, A., Ochsenbein, F., Stenholm, B., Tylenda, R., Marcout, J., Schon, C., 1992, The Strasbourg-ESO catalogue of Galactic Planetary Nebulae
Aller, L. H., Keyes, C. D., 1987, ApJS, 65, 405
Barlow, M. J., 1987, MNRAS, 227, 161
Blöcker, T., 1995, A&A, 299, 755
Ciardullo, R., 1995, in IAU Highlights of Astronomy Vol. 10, ed. I. Appenzeller I., Dordrecht, Kluwer, p. 507
Ciardullo, R., Jacoby, G. H., Ford, H. C., Neill, J. D.,1989, ApJ, 339, 53
Dopita, M. A., Meatheringham, S. J., Webster, B. L., Ford, H. C., 1988, ApJ, 327, 639
Dopita, M. A., Meatheringham, S. J., 1991, ApJ, 377, 480
Dopita, M. A., Jacoby, G. H., Vassiliadis, E., 1992, ApJ, 389, 27
Dopita, M. A., Vassiliadis, E., Wood, P. R., Meatheringham, S. J., Harrington, J. P., Bohlin, R. C., Ford, H. C., Stecher, T. P., Maran, S. P., 1997, ApJ, 474, 188
Ford, H. C., 1983, Planetary Nebulae, IAU Symp. 103, ed. D. R. Flower, Reidel, p. 443
Forestini, M., & Charbonnel, C., 1997, A&AS, 123, 241
Górny, S. K. G., Tylenda, R., Szczerba, R., 1994, A&A, 284, 949
Henry, R. B. C., 1989, MNRAS, 241, 453
van den Hoek, L. B., Groenewegen, M. A. T., 1997, A&AS, 123, 305
Jacoby, G. H., 1989, ApJ, 339, 39
Jacoby, G. H., 1998, Planetary Nebulae, IAU Symp. 180, eds. H. Habing & H. Lamers, Reidel, Kluwer, p. 448
Jacoby, G. H., Kaler, J. B., 1993, ApJ, 417, 209
Kaler, J. B., Jacoby, G. H., 1991, ApJ, 382, 134
Kingsburgh, R. L., Barlow, M.J., 1994, MNRAS, 271, 257
Leisy, P., & Dennefeld, M., 1996, A&AS, 116, 95
Mc Call, M. L., Richer, M. G., Stasińska, G., 1998 (in preparation)
Méndez, R. H., Soffner, T., 1997, A&A, 321, 898
Méndez, Kudritzki, R. P., Ciardullo, R., Jacoby, G. H., 1993, A&A, 275, 534
Monk, D. J., Barlow, M. J., Clegg, R. E. S., 1988, MNRAS, 234, 583
Peimbert, M., 1985, Rev Mex A&A, 10, 125
Peimbert, M., Torres-Peimbert, S., 1983, in Planetary Nebulae, symp. IAU 103, ed. D. R. Flower, Reidel, p. 233
Ratag, M. A., Pottasch, S. R., Dennefeld, M., Menzies, J., 1997, A&AS, 126, 297
Richer, M. G., 1993, ApJ, 415, 240
Richer, M. G., Mc Call, M. L., 1995, ApJ, 445, 642
Richer, M. G., Mc Call, M. L., Arimoto, N., 1997, A&AS, 122, 215
Richer, M. G., Stasińska, G., Mc Call, M. L , 1998a (submitted)
Richer, M. G., Mc Call, M. L., Stasińska,G., 1998b (submitted)
Stasińska, G., Tylenda, R., Acker, A., Stenholm, B., 1991, A&A, 247, 173
Stasińska, G., Tylenda, R., Acker, A., Stenholm, B., 1992, A&A, 266, 486
Stasińska, G., Tylenda R., 1994, A&A, 289, 225
Stasińska, G., Leitherer, K., 1996, ApJS, 107, 661
Stasińska, G., Górny, S. K. G., Tylenda, R., 1997, A&A, 327, 736
Stasińska, G., 1998 (in preparation)
Vassiliadis, E., Wood, P. R., 1994, ApJS 92, 125
Vigroux, L., Stasińska, G., Comte, G., 1987, A&A, 172, 15
Webster, B. L., 1988, MNRAS, 230, 377
Worthey, 1996, in From Stars to Galaxies: The Impact of Stellar Physics on Galaxy Evolution, ASP Conference Series 98, ed. C. Leitherer, U. Fritze-von Alvensleben, & J. Huchra (Astronomical Society of the Pacific: San Francisco), p. 467